The Osteochondral Interface as a Gradient Tissue: From Development to the Fabrication of Gradient Scaffolds for Regenerative Medicine

The Osteochondral Interface as a Gradient Tissue: From Development to the Fabrication of Gradient Scaffolds for Regenerative Medicine

Andrea Di Luca*[1], Clemens Van Blitterswijk[1,2], and Lorenzo Moroni[1,2]

The osteochondral (OC) interface is not only the interface between two tissues, but also the evolution of hard and stiff bone tissue to the softer and viscoelastic articular cartilage covering the joint surface. To generate a smooth transition between two tissues with such differences in many of their characteristics, several gradients are recognizable when moving from the bone side to the joint surface. It is, therefore, necessary to implement such gradients in the design of scaffolds to regenerate the OC interface, so to mimic the anatomical, biological, and physicochemical properties of bone and cartilage as closely as possible. In the past years, several scaffolds were developed for OC regeneration: biphasic, triphasic, and multilayered scaffolds were used to mimic the compartmental nature of this tissue. The structure of these scaffolds presented gradients in mechanical, physicochemical, or biological properties. The use of gradient scaffolds with already differentiated or progenitor cells has been recently proposed. Some of these approaches have also been translated in clinical trials, yet without the expected satisfactory results, thus suggesting that further efforts in the development of constructs, which can lead to a functional regeneration of the OC interface by presenting gradients more closely resembling its native environment, will be needed in the near future. The aim of this review is to analyze the gradients present in the OC interface from the early stage of embryonic life up to the adult organism, and give an overview of the studies, which involved gradient scaffolds for its regeneration.

Birth Defects Research (Part C) 105:34–52, 2015.

Key words: osteochondral tissue; regenerative medicine; gradient; 3D scaffolds

Introduction

Osteoarthritis (OA) nowadays represents worldwide, a common degenerative disease in old people with a high socio-economic impact. It has been estimated that 40% of the population over 65 years presents symptomatic OA in large joints, consequently affecting the quality of life of elderly populations (Dunlop et al., 2001; Mannoni et al., 2003; Dawson et al., 2004). The increase of life expectancy will eventually increase the percentage of population presenting OA. Clinically, current therapies to regenerate osteochondral (OC) tissues are not yet completely successful. All the available treatments such as reparative surgery, allografts, autografts, and the implantation/transplantation of autologous chondrocytes, besides limitations like the formation of fibrocartilage and lack of donor supply, inflict further tissue damage before any therapeutic effect can be achieved (Schaefer! et al., 2000; Martin et al., 2007). Due to the fore-mentioned reasons, major efforts in regenerative medicine have been placed in the past few years to present new solutions that hold the potential to improve the outcome of current therapies. Scaffold-based regenerative medicine strategies, in particular, have found a lot of applications in the past decades in skeletal tissue engineering, due to their ability to support cells and tissue growth in 3D and to mimic to some extent the extracellular matrix (ECM) architectural properties and composition.

The OC tissue is located at the end of long bones and allows the transition from bone to cartilage. Since these two anatomical structures present significantly different characteristics at the macroscales, microscales, and nanoscales in terms of structural, mechanical, physicochemical, and biological properties, an interfacial tissue that shows a gradual variation of these features at different scales is necessary. Due to the fine interplay between the bone and the cartilage side, the two compartments cannot be separated, since they are tightly interconnected not only under physiological conditions, but also during the progression of OA. When thinking about the regeneration of the OC tissue, designing scaffold-based regenerative strategies that can take into consideration such graded variations of the native tissue properties seems, therefore, a promising route. In the past few years, a number of scaffolds presenting either a biphasic or triphasic (Schek et al., 2004; Grayson et al., 2010; Aydin, 2011, Kon et al., 2011; Levingstone et al., 2014; Shimomura et al., 2014) structure were proposed for the regeneration of the OC tissue *in vitro* and

[1]Tissue Regeneration Department, University of Twente, 7522 NB Enschede, The Netherlands
[2]Maastricht University, MERLN Institute for Technology Inspired Regenerative Medicine, Complex Tissue Regeneration Department, Maastricht, ER 6229, The Netherlands

*Correspondence to: Andrea Di Luca, University of Twente, Tissue Regeneration Department, Drienerlolaan 5,7522 NB, Enschede, The Netherlands. E-mail: adiluca84@gmail.com

We would like to acknowledge STW (gran number 11135) for funding.

Published online 16 March 2015 in Wiley Online Library (wileyonlinelibrary.com). Doi: 10.1002/bdrc.21092

in vivo. Constructs presenting a discrete or continuous gradients in geometry (Woodfield et al., 2004), stiffness (Levingstone et al., 2014), biochemical composition (Benders et al., 2013; Levingstone et al., 2014) at the macroscale and microscale, as well as gradients in growth factor concentrations (Singh et al., 2008; Oh et al., 2011; Zhang et al., 2012), can be found in literature. The aim of this review is to dissect the gradient nature of the OC tissue, such as its changes in ECM molecular composition and orientation, the resulting variation in physicochemical and mechanical properties, as well as in the cellularity, nutrient availability, and growth factors involved in its development, This knowledge is then linked to the strategies applied so far in regenerative medicine for OC tissue regeneration.

OC Tissue Development

From a developmental point of view, bone and cartilage of appendicular bones arise from the lateral plate mesoderm. The first step in their development is the condensation of OC progenitor cells into aggregates under the effect of transforming growth factor (TGF-β), which promotes the expression of molecules involved in the condensation process such as N-cadherin, neural cella adhesion molecule (N-CAM), fibronectin, and Tenascin-C (Chimal-Monroy and Diaz de Leon, 1999; Kronenberg, 2003). The condensation determines the formation of a central part of cells, which continue to proliferate and express the transcription factor sex determining region Y-box 9 (sox-9), and a population of cells located in the periphery of the aggregates known as the perichondrium (Nakashima and de Crombrugghe, 2003). Sox-9 is expressed in all the chondrocytes with the exception of hypertrophic chondrocytes (de Crombrugghe et al., 2001). The perichondrium functions as a reservoir of chondrocytes during bone development, which will progress until bone formation. Under the influence of a growth factor cocktail, including amongst others insulin growth factor-1, fibroblast growth factor-2, and bone morphogenetic proteins (BMPs) -2, -4, -7, and -14 (Kronenberg, 2003; Pogue and Lyons, 2006; Wang et al., 2011), the cells within the aggregates proceed to chondroblasts and begin to produce aggrecan and collagen type II, IX, and XI. Chondroblasts organize into a structure called growth plate, from which bone will be generated. The central part of the growth plate is called the primary ossification center and constitutes the first cartilage portion replaced by bone. The growth plate is responsible for the growth in length of appendicular bones during life. Within the growth plate different zones can be identified, each one characterized by a pool of chondrocytes displaying differences in size, proliferation rate, and ECM deposition. At the distal end of long bones, chondrocytes appear small and rounded. Chondrocytes are located in the so called resting zone, which has the function of providing further cells that will continue in the maturation process. Once stimulated, resting zone chondrocytes interact with the surrounding ECM, assume a flat phenotype, and begin the formation of the columnar zone. Near the top of the columnar zone, cells display the highest proliferation rate (Smits et al., 2004). Cell proliferation is maintained by the action of parathyroid hormone-related peptide (PTHrP), which is produced by periarticular chondrocytes and negatively regulates terminal cell differentiation (Kobayashi et al., 2002; Kronenberg, 2003). As we move from the periarticular zone into the resting and columnar zones, chondrocytes move away from the PTHrP source, arrest their proliferation, and undergo prehypertrophic differentiation at the bottom of the columnar zone. Prehypertrophic chondrocytes produces Indian hedgehog (IHH), which stimulates on one side PTHrP synthesis by periarticular chondrocytes, and on the other side cell terminal differentiation and hypertrophic zone formation. Their volume increases by 20-fold (Goldring et al., 2006) and their ECM synthesis switches from mainly collagen type II to collagen type X formation. The furthest chondrocyte developmental stage is the late hypertrophic chondrocyte, which expresses some preosteoblast markers such as matrix metalloproteinase (MMP-13), known to promote vascular invasion and the consequent progressive replacement of cartilage by bone. Late hypertrophic chondrocytes represent the terminal stage of differentiation in the chondrogenic cell lineage (Pacifici et al., 1990). The final fate of hypertrophic chondrocytes is apoptosis, but cells which escape death become osteoblasts (Bianco et al., 1998). The cells of the perichondrium flanking the hypertrophic zone become osteoblasts and form the periosteum, under the effect of Runt-related transcription factor 2 (Runx-2). The hypertrophic chondrocyte begins to express Runx-2, an early marker for osteogenesis and continue to be expressed in osteoblasts. Blood vessel and osteoblasts from the newly formed bone invade the hypertrophic region and replace cartilage with bone and bone marrow (Kronenberg, 2003).

Many of the events in chondrogenesis, from early differentiation of hMSCs in prechondrocytes to the evolution toward the hypertrophic stage, are governed by the Wnt signaling pathway. This pathway can follow two distinct routes named Wnt “canonical” and “noncanonical” pathways. In the β-catenin or canonical pathway, Wnt binds its receptor Frizzled, which activate glycogen synthase kinase-3β (GSK-3β) that determines the phosphorylation of β-catenin. In its phosphorylated form, β-catenin is stable and accumulates in the cytoplasm. Subsequently, β-catenin translocates to the nucleus and interacts with the gene expression regulatory apparatus (Yates et al., 2005). The noncanonical pathway is β-catenin independent and based on intracellular calcium levels. The binding of Wnt with Frizzled stimulates the release of intracellular Ca^{++} and the activation of protein kinase C and Ca^{2+}-calmodulin-dependent protein kinase II, which are involved in ventral patterning and regulation of cell adhesion, migration, and

tissue separation (Kühl et al., 2000; Komiya and Habas, 2008). In contrast to what happens in the growth plate, articular cartilage is highly resistant to the hypertrophic differentiation (Leijten et al., 2012). The control of chondrocyte differentiation relies on the expression of antagonists of the Wnt signaling pathway such as Gremlin 1, Frizzled-Related Protein, and Dickkopf-1 (Dkk-1; Kawano and Kypta, 2003). Beside the Wnt family, another pool of proteins actively involved in chondrogenic and osteogenic development is represented by the transforming growth factor β (TGF-β) superfamily. Within the TGF-β superfamily, BMPs and TGF-βs are the most important growth factors known to regulate osteogenic and chondrogenic cell differentiation (Chen et al., 2012). There are three TGF-β isoforms, namely TGF-β 1, 2, and 3. TGF-β1 and TGF-β3 are related to chondrogenesis. The effectors of the canonical pathways are the small mothers against decapentaplegic proteins (Smads), a pool of cytoplasmic proteins able to form complexes which translocate in the nucleus and act as transcription factors (Heldin et al., 1997). Smad-1, -2, -3, -5, and -8 are effectors of the TGF-β and BMP pathways. Smad-4 acts as cofactor, forming the complex, which translocate in the nucleus, whereas Smad-6 and -7 have an inhibitory activity (Itoh et al., 2001). In TGF-β pathway, one TGF-β isoform binds a type II dimeric receptor, which recruits a dimeric type I receptor generating a heterotetrameric complex. This complex presents a kinase intracellular domain, type II receptor phosphorylates type I receptor (Heldin et al., 1997), which phosphorylates Smad-2 or Smad-3. This event causes the formation of the Smad2/3-Smad4 complex, its translocation in the nucleus and the action as transcription factor, increasing the Sox9-dependent transcriptional activity and the transcription of collagen type IIα1 (Furumatsu et al., 2005; Lin et al., 2005). BMP family also consists of several isoforms. BMP-2, -6, and -7 are known to promote osteogenic differentiation whereas BMP-3 act as an inhibitor. The BMP pathway presents the same event sequence. The BMP binds a heterocomplex composed of a type I and a type II receptor. Binding generates the recruitment of other, in order to form the heterotetrameric complex. Type II receptor phosphorylates type I receptor, which phosphorylates Smad-1, -5 or -8 (Mundy, 2006). This event causes the formation of the Smad-1/5/8-Smad-4 complex, which translocates into the nucleus determining the transcription of Runx2, collagen typeIα2, alkaline phosphatase, and osteocalcin (Mundy, 2006).

The Components of OC Tissue

The OC tissue is composed by two main compartments, subchondral bone and articular cartilage (Kwan et al., 2009). Within these compartments, a further division in areas can be performed. Beside the subchondral bone plate, the calcified cartilage is often considered part of it; the line defining the passage to the articular cartilage is the so-called tide mark. Articular cartilage can be further divide into three regions: (i) the radial zone, standing on top of mineralized cartilage; (ii) the transition zone, central in the cartilage tissue; (iii) and the superficial zone, interfacing with the synovial fluid and the joint space. The OC tissue has an height of $\sim$3 mm in adults, of which about 90% consists of articular cartilage, 5% calcified cartilage, and 5% the subchondral bone plate (Hunziker et al., 2002). A schematic representation and histological section of the components of the OC tissue are shown in Figure 1.

SUBCONDRAL BONE AND CALCIFIED CARTILAGE

Long bones are divided into diaphysis, being the central part of the bone, and the epiphysis, localized in proximity of the joints. The structure of bone in the two compartments differs by the radial variation of bone compactness. In the diaphysis, a zone of more compact bone, called cortical bone, can be identified in the external part. Cortical bone presents a porosity ranging from 5 to 30% and a bone volume fraction ranging from 85 to 90%. Moving towards the center, a more porous structure, called cancellous or trabecular bone, is encountered. The porosity of trabecular bone ranges from 30 to 90% and its bone volume fraction from 5 to 60%. Bone volume fraction decreases when moving toward the bone marrow channel, in which the space between the trabecula is wider and filled with the bone marrow. The subchondral bone in the epiphysis presents similar characteristics of the trabecular bone with bone volume fraction ranging from 6 to 36%, a trabecular thickness of 100–190 μm, a trabecular concentration ranging from 0.61 to 2.06 trabecules/mm, and the space between them ranging from 320 to 1670 μm (Bobinac et al., 2003). At the epiphysis, the compact bone is reduced to a thin layer. The subchondral bone serves to keep the integrity of the overlying articular cartilage (Sharma et al., 2013). At the molecular and cellular level, bone and cartilage differ significantly from each other. Bone ECM is mainly based on collagen type I collagen fibrils with mineral deposits of calcium and phosphate, called hydroxyapatite (HA). Beside collagen, other structural proteins are present. Among them the most important are osteopontin, thrombospondin, and bone sialoprotein for cell and HA attachment, and osteocalcin and osteonectin for the binding of HA and calcium respectively (Heinegard and Oldberg, 1989). Being a vascularized tissue and due to the presence of the bone marrow, the cell composition of bone is very heterogeneous. Within the bone marrow, a small fraction (0.002%) is represented by mesenchymal stromal/stem cells (hMSCs), which are the precursor, among others, of osteoblasts, osteoclasts, and chondrocytes. Osteoblasts are the cells responsible for HA synthesis, and deposition. Osteoclasts have an opposite activity, being responsible for bone resorption. Beside their structural function, bones represent the reservoir of

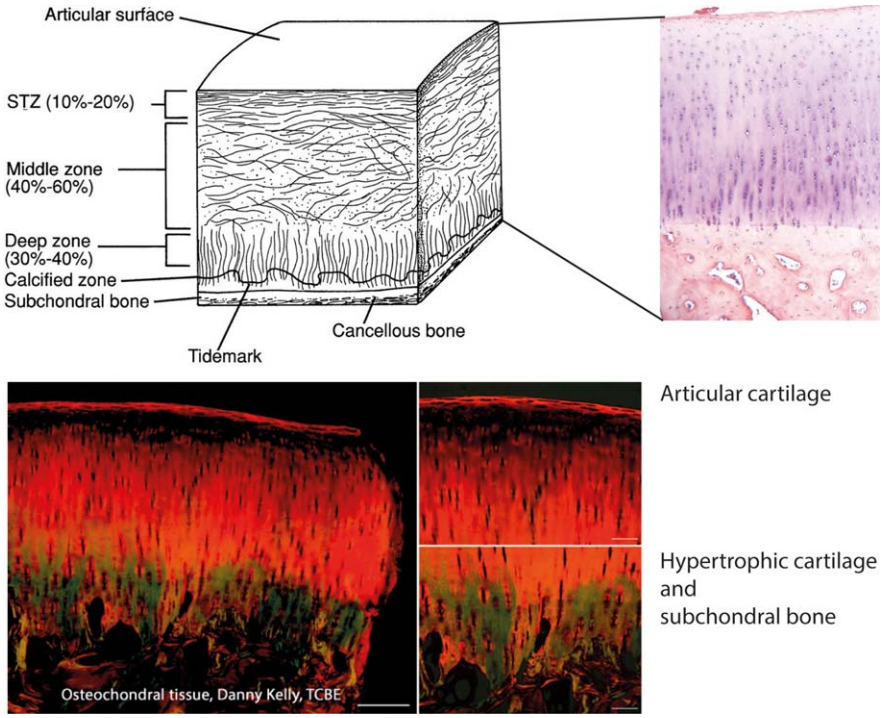

FIGURE 1. *Schematic representation of the osteochondral tissue and its components and osteochondral tissue from two histological sections. Modified from Buckwalter, 1994, Kwan Tat , 2009, and https://www.tcd.ie/biosciences/gallery/.*

calcium for the human body. The activity of osteoblasts and osteoclasts is fine-tuned by hormones depending on the request of calcium from the body, which results in a process of bone synthesis and remodeling through the whole life of an individual (Harada and Rodan, 2003). The interplay between osteoblasts and osteoclasts is further controlled by osteocytes, the most abundant cell in bone tissue (Knothe Tate et al., 2004). Besides being actively involved in maintaining the bony matrix, the osteocytes are also mechanotransductors. Their immersion in the bone matrix and connection with adjacent osteocytes in the canaliculi allows exogenous and endogenous signals to be transmitted via mechanical, electrical, and chemical mechanisms (Knothe Tate et al., 2004). Another cell type present in this tissue is the endothelial cells forming the blood vessels, which run through the bones. Moving from the epiphysis toward the joint, the first portion of the cartilage encountered is the calcified zone. It is considered together with the subchondral bone, since it is a transition portion presenting some characteristics of the cartilaginous tissue, such as the deposition of collagen type X, and some characteristics of the bone tissue, such as the presence of alkaline phosphatase and of mineral deposits. Its function is to provide a good attachment between bone and cartilage, and transfer the forces from the joint to the subchondral bone (Oegema, 1997).

ARTICULAR CARTILAGE

The function of articular cartilage is to transfer and distribute the load forces to the subchondral bone; the disposition and localization of structural proteins such as collagen and proteoglycans is optimized to perform this function. Collagen type II, in particular, is the most abundant component of the ECM in hyaline cartilaginous tissue. Another abundant component of the ECM is the proteoglycans, responsible for the water uptake and osmolarity maintenance. There are two classes of proteoglycans, large aggregating proteoglycans such as aggrecan and smaller ones, such as decorin, biglycan, and fibromodulin (Bhosale and Richardson, 2008). Articular cartilage can be divided into three main zones: moving from the articular surface to the subchondral bone, the superficial, the transitional, and the radial or deep zones. The superficial and transitional zones each constitute 10% of the height of the articular cartilage layer. The radial zone represents instead the bulk of articular cartilage, accounting for 80% of it (Hunziker et al., 2002). Chondrocytes represent the 2% of the component of the articular cartilage, and they are the only cell type present in this tissue. Chondrocytes are characterized by a round shape, different size and orientation along the cartilage height, and are surrounded by two main ECM proteins, namely collagen type II and aggrecan. Chondrocytes are fairly small cells, presenting a diameter of 13 μm, a surface area of 821 μm^2, and a volume of 1,748 μm^3, approximately. These features do not vary much among the cartilage zones, with the exception of the hypertrophic one (Hunziker et al., 2002). When a chondrocyte becomes hypertrophic, its volume increases up to 20 times (Farnum et al., 2002) and starts to produce collagen type X. Chondrocytes are organized in chondrons which

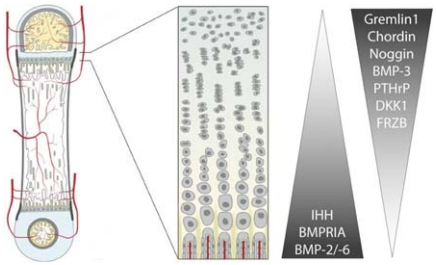

FIGURE 2. *Schematic representation of the growth plate and the gradients formed by growth factors. The arrow direction describes a descendent gradient. Modified picture from http://serkadis.net/.*

are the primary structural, functional and metabolic unit in hyaline cartilage. A chondron comprises the chondrocyte and the pericellular molecular environment of which collagen type VI and IX are the major components. These ECM proteins are present only in close proximity of the cell, while they decrease to very low levels in the cartilage matrix. Beside an axial characterization of the matrix, another distinction can be done, based on the matrix between one chondron and the following one. Close to the chondrocyte the pericellular matrix is rich in collagen types VI and IX, as mentioned above, with the addition of proteoglycans such as hyaluronan (Mason, 1981), sulfated proteoglycans (Poole et al., 1984), and biglycans (Miosge et al., 1994) as well as matrix glycoproteins such as fibronectin (Glant et al., 1985), link protein (Poole, 1997), and laminin (Durr et al., 1996). Moving away from the chondrocyte and its pericellular matrix, the territorial zone is encountered, which is rich in chondroitin sulfate. Further away, in the space between chondrons, the inter-territorial matrix is localized in which the main proteoglycans are rich in keratan sulfate (Poole, 1997). In the superficial and transitional zone, chondrons are exclusively single cells units, whereas in the radial zone they contain on average 5–8 chondrocytes (Hunziker et al., 2002).

Moving from the radial to the transitional zone, the ECM maintains the same composition and presents decorin as proteoglycan, in addition to aggrecan. In this region, collagen fibers pass from a vertical to a more horizontal orientation. The surface zone of articular cartilage is the one responsible for the lubrication of the joint. Its ECM is mainly composed by collagen type I (Blitterswijk), collagen type II, and lubricin or PRG4, a proteoglycan present also in the synovial fluid responsible for joint lubrication and synovial homeostasis (Musumeci et al., 2014). The collagens are responsible for the strength and the high shear stress resistance of the superficial layer (Buckwalter et al., 1994). Here, collagen fiber orientation progresses toward a completely horizontal configuration, which contributes to the low friction mechanical properties of hyaline cartilage.

THE OC TISSUE AS A GRADIENT TISSUE

GRADIENTS IN OC DEVELOPMENT

During development, a rich orchestration of growth factors act at different levels within the growth plate spatially and temporally (Fig. 2). To ensure the proliferation of progenitor cells on the superficial layer, but prevent it in the lower part, a PTHrP gradient is formed. “Elder cells” move downwards and keep dividing, as long as the PTHrP effect is present. Once they reach the lower resting phase of the growth plate, the effect is no longer present, and this makes them proceed toward the next step of maturation. Similarly, once the chondrocytes have reached the hypertrophic stage, BMP signaling plays a major role in bone formation. The BMP effect is determined by a combination of cell susceptibility and BMP antagonist. BMP-2 and -6 are produced by osteoblasts and hypertrophic chondrocytes. Their expression is higher in the hypertrophic zones, and decreases while moving upward in the resting and proliferative zones. Their effect also decreases from the hypertrophic zone toward the proliferation and resting zones, since the expression of their receptor BMPRIA follows the same trend (Nilsson et al., 2007). The activity of BMPs is finely regulated, in order to stimulate the right portion of the growth plate, and therefore an opposite gradient of BMPs antagonists can be found. BMP-3 is considered an antagonist, since its action inhibits BMP stimulated bone formation (Gamer et al., 2008). Among the antagonists, noggin, gremlin, chordin, and BMP-3 are more highly expressed in the resting zone compared to the proliferative and hypertrophic ones (Nilsson et al., 2007), thus resulting in an increased gradient of osteoinductive signals within the growth plate. The development of chondrocytes toward the hypertrophic state is finely tuned via the expression of antagonists, such as Gremlin 1, Frizzled-Related Protein, and Dkk-1. Their expression presents a decreasing trend from the resting zone, in which their presence is the highest toward the hypertrophic zone in which their levels are the lowest (Leijten et al., 2012).

STRUCTURAL GRADIENT–FIBRILS AND ECM COMPOSITION

Due to its compartmental architecture, the OC tissue presents a variety of axial gradients along its structure. In the OC tissue, the structural gradient is defined by the composition and organization of the ECM (Figs. 1 and 3). As mentioned earlier, the subchondral bone is a mineralized tissue comprised primarily of collagen type I and HA. HA, the inorganic component of subchondral bone, comprises $85.8\% \pm 3.4\%$ of its dry weight, decreasing to $65.1\% \pm 2.3\%$ in the calcified cartilage to completely disappear in the hyaline cartilage (Zhang et al., 2012). Collagen type I is present in bone and starts to decrease in content from the mineralized cartilage. In cartilage, collagen type I can be found only in the surface layer. In the mineralized cartilage lying above subchondral bone, the

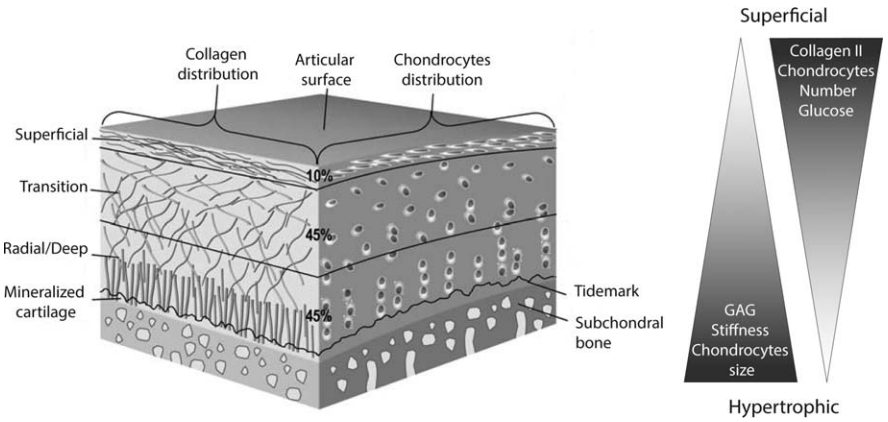

FIGURE 3. *On the left side, schematic representation of the osteochondral tissue. On the right side, directions of its gradients. The stiffness gradient continue in the subchondral bone, whereas the nutrient gradient stops in the radial zone. Modified from Woodfield, 2005.*

residing cells are a particular type of chondrocytes named hypertrophic chondrocyte, which present the peculiar characteristic of producing collagen type X, and are embedded in mineralized ECM. In this deep zone of the OC tissue, the direction of the fibrils do not play a major role, since the integrity and the shock absorption ability is given by the mineralization of the ECM and the presence of collagen type X. Collagen type II starts to appear in the radial zone in thick fibers, with a direction that is perpendicular to the articular surface. From the radial zone moving towards the superficial zone, mineralization also disappears. In the transitional zones, collagen type II fibers increase in number, but decrease in diameter and assume a more parallel direction, to become totally parallel to the articular surface in the superficial zone. This direction determines the greatest tensile and shear strength (Bhosale and Richardson, 2008). Conversely, the amount of glycosaminoglycans (GAGs) forms a gradient opposite to the one generated by the collagen, decreasing from the radial zone toward the joint surface. GAGs are responsible for the gradient in stiffness within articular cartilage: as the total proteoglycan concentration decreases, the compressive stiffness also decreases (Mansour).

CELLULARITY GRADIENT AND PERICELLULAR ENVIRONMENT

A variety of cells are present in the OC tissue. As previously described, the subchondral bone is comprised of osteoblasts for collagen and mineral deposition, osteoclasts for bone remodeling, and calcium mobilization, and osteocytes for their regulation and mechanotransduction (Knothe Tate et al., 2004). Being highly vascularized, bone contains endothelial cells composing the vascular network, which is missing in articular cartilage, due to its typical avascular nature. The variation from bone to cartilage tissue in terms of cells does not follow a gradient. However, within the cartilage tissue a gradient in cell distribution, size, and deposited pericellular matrix can be observed. Within cartilage, the only cell type present has been always believed to be chondrocytes. Although defined as chondrocytes throughout the tissue, this simplification is misleading since profound differences are present in the behavior, morphology, and function of these cells among the cartilage zones. Chondrocytes vary in number, size, and disposition, depending in which region they are located. The gradient in chondrocyte density per zone can be summarized by a variation from 7,000 to 24,000 cells/mm^3 (Fig. 3). Beside the variation in cell number, chondrocyte appearance varies in a gradient way. The cell body decreases in size from the hypertrophic zone toward the superficial layer. In addition, the morphological and functional units of hyaline cartilage, the chondrons, display a gradient through the cartilage layers. In the radial zone, chondrons are arranged in columns. Even if chondrocytes have the characteristic of no direct cell-cell connections, the tails of the chondrons are entangled, in order to guarantee continuity from one chondron to the following one. The number of chondrocytes per chondron is estimated to change from one to eight, with the lowest number in the superficial zone and the highest in the radial zone (Hunziker, 2002; Hunziker et al., 2002). Moving toward the articular surface, as the chondrocytes/chondron number decreases to one, the overall number of chondrocytes increases. Their appearance passes from column like structures to single entities dispersed in the ECM. An additional switch in cell number, function, and morphology can be seen from the transition to the superficial region of the articular cartilage. The collagen produced by these cells changes from collagen type II to collagen type I. Their morphology change from rounded to flat and they form a superficial cell layer with a very low amount of ECM separating them from each other. Additionally, the superficial region is the area with the highest proliferative rate (Blitterswijk et al., 2002). From a developmental point of view, the maturation of chondrocytes follows an opposite trend compared to the cell density. Hayes et al. (2001) reported that the development of chondrocytes follows an appositional direction. The cartilage progenitor cells are located in the superficial region, and their development is shown to pass through the cell phenotypes encountered from the

superficial to the deep region. Eventually, the chondrocyte would enter in the hypertrophic stage, which is thought to be the last stage of their development (Pacifici et al., 1990).

STIFFNESS GRADIENT

From the subchondral bone, the mineralization and stiffness of the ECM decreases when moving toward the articular surface, as shown in Figure 3. This can be defined as a discrete gradient, since the subchondral bone and the mineralized cartilage present the highest amount of minerals that disappear completely in the other zones composing the articular cartilage. The subchondral bone has an elastic modulus of 3.9 ± 1.5 GPa, which decreases in the mineralized cartilage to 0.32 ± 0.25 GPa (Mente and Lewis, 1994). From the mineralized cartilage region moving towards the articular surface, the stiffness decreases from 0.6 $6\pm$ 0.05 MPa in the deep zone to 0.24 ± 0.05 MPa in the superficial zone (Rolauffs et al., 2010). Articular cartilage has also the peculiarity to change its mechanical properties when a loading is applied dynamically. Due to its highly viscoelastic character, its dynamic stiffness increases with increasing the loading frequency, spanning from 4 to 10 MPa (Treppo et al., 2000; Moroni et al., 2006). The final load is borne by the bone and the cartilage has the function to transfer the forces through the ECM.

NUTRIENTS/O_2 GRADIENT

The bone side of the OC tissue is reached by blood vessels that are responsible for bone nutrient supply and waste removal. One of the major anatomical characteristics of cartilage, instead, is the absence of blood vessels through the entire width. Nutrients are transported to the cells mainly by diffusion from the synovial fluid. Nutrient transport is also sometimes thought to be assisted by movement of fluid in and out of cartilage in response to cyclic loading of the tissue (O'Hara et al., 1990). Therefore, gradients of nutrients and metabolic byproducts exist through cartilage due to the balance between transport and rates of cellular metabolism (Zhou et al., 2008). This process is aided by the presence of proteoglycans that have the ability of retaining water, which flows in with the nutrients during loading relaxation and flows out with the metabolites during compression. Among the nutrients, glucose represents the primary source of energy. Pyruvate, the product of glycolysis, is converted in acetyl coenzyme A, which is the main supplier of carbon in Krebs cycle. A glucose gradient from the synovial fluid toward the deep zone of cartilage is also present as shown by Zhou et al. (2008). Glucose is not only the most important source for energy production, but also a key component in GAG synthesis. It has been shown that across cartilage from the synovial side to the subchondral bone, a glucose gradient exists (Prydz and Dalen, 2000; Fig. 3). Similar to glucose, the oxygenation of cartilage comes from the synovial fluid. Therefore, a gradient of oxygen is formed from the joint of the surface toward the radial zone (Fig. 3). The oxygen tension of synovial fluid in humans is 6.5–9.0% (50–70 mm Hg; Falchuk et al., 1970; Lund-Olesen, 1970). Measured oxygen tension in articular cartilage ranges from 7% (53 mm Hg) in the superficial layer, to $<1\%$ (7.6 mm Hg) in the deep zone (Silver, 1975; Fermor et al., 2007) of the oxygen tension of synovial fluid.

Gradient Scaffolds for OC Regeneration

GENERAL REQUIREMENTS

In the past few years, the number of publications involving scaffolds addressing the gradient nature of the OC tissue has greatly increased. Studies involving structural porosity gradient were proven to increase the cell seeding efficiency of human osteosarcoma cell line SaOs-2 (Sobral et al., 2011) and to mimic *in vitro* the gradient structure of the cartilage in terms of chondrocytes and ECM distribution (Woodfield et al., 2005). In the literature, it is possible to find several studies aiming at the treatment of articular cartilage alone or at the development of biphasic scaffolds for the treatment of bone and cartilage as separate tissues. Due to the wide range of gradients present in the OC tissue, several choices can be made in terms of gradient scaffolds. Typically, biphasic or triphasic scaffolds have been developed, displaying either discrete or continuous gradients (Singh et al., 2010, Mohan et al., 2011, 2014; Elizaveta Kon, 2014). To define biphasic or triphasic scaffolds, different materials can be chosen. In this respect, the selection of biomaterials needs to take into account not only their biocompatibility, but also the effect that each material will play on the seeded cells (Tables 1 and 2). For the scaffold preparation, natural or synthetic polymers can be used. A logical criteria for the selection of natural polymer candidates passes through the components of the ECM. For the bone compartment, collagen type I combined with HA was used to produce scaffolds or to cover the underlying polymer by coating the pore surface (Aydin, 2011), to mask the synthetic polymer and present an ECM like environment for cell attachment, growth, and differentiation. For the regeneration of the cartilage portion, collagen type II, glycosaminoglycans, and hyaluronic acid have been used (Zhao et al., 2013). For both bone and hyaline cartilage, the most common synthetic polymers used are poly(lactic acid) (PLLA; Solchaga et al., 2005), poly(glycolic acid) (PGA; Aydin, 2011), and polycaprolactone (PCL; Ding et al., 2013).

Among other properties, an OC scaffold should be biodegradable with a degradation rate matching the rate of ECM production, and should have high levels of porosity and pore interconnectivity for cell attachment, and gas, nutrient, and waste products exchange, (Aydin, 2011). The mechanical properties of the fabricated scaffolds should match the gradient in mechanical properties present in the

TABLE 1. *Summary of the Biphasic Scaffolds Described, Indicating the Biomaterials, Cells, and Growth Factors used and the Main Results for Each Construct*

Author	In vitro/in vivo	Material subchondral bone + cells	Material cartilage + cells	Main findings
Schaefer et al., 2000	In vitro	PGA nonwoven meshes; chondrocytes	PLGA/PEG foams, Periosteal cells	Increased ECM mineralization, GAG synthesis, integration with subchondral bone
Schek et al., 2004	In vivo, nude mice	HA ceramic Fibroblasts expressing BMP-7	PLLA sponge Chondrocytes	Bone and blood vessel, mineralized transition tissue, Cartilaginous tissue
Cao et al., 2003	In vitro	Plotted PCL Stromal cells from iliac crest	Plotted PCL Rib cartilage chondrocytes	Bone like tissue formation Cartilage-like ECM
Ding et al., 2013	In vivo, nude mice	Plotted PCL + HA + MSC	PGA/PLA nonwoven fibers + chondrocytes	Osteogenic and chondrogenic markers, interface with hypertrophic cartilage
Kandel et al., 2006	In vivo, sheep	CPP	Chondrocyte layer	OC regeneration, some sign of cartilage maturation
Duan et al. (in press)	In vivo, rabbit	Salt leached PLGA 300-450 μm + MSC	Salt leached PLGA 100-200 μm + MSC	Simultaneous regeneration of articular cartilage and subchondral bone
Chen et al., 2012	In vivo, rabbit	BMP-2-activated HA/chitosan-gelatin	TGF-β1-activated chitosan-gelatin	Regeneration of articular cartilage and subchondral bone
Re'em et al., 2012	In vivo, rabbit	alginate-sulfate, alginate, 0.18%D-gluconic acid/hemicalcium salt + BMP4	alginate-sulfate, alginate, 0.18%D-gluconic acid/hemicalcium salt + TGF-β1	ECM composition of hyaline cartilage with no signs of mineralization, new formed woven bone in the bottom part

OC tissue, with a stiffer scaffold for the bone compartment and a gradually softer scaffold for the cartilage compartment. Additionally, the inner geometry of the construct must be taken into consideration, ideally mimicking the structural and architectural properties of the native tissue.

CHOOSING CELLS

After considering general design criteria in fabricating a scaffold for OC regeneration, one should consider whether the scaffold will be directly implanted or seeded with cells before implantation. In the latter case, two main solution have been proposed: (i) the direct use of already differentiated cells (Cao et al., 2003; Martin et al., 2007; Jeon et al., 2014) or (ii) the use of progenitor cells, namely MSCs from different sources (Heymer et al., 2009; Grayson et al., 2010). When differentiated cells are used, the part of the scaffold, which will be in contact with the subchondral bone is loaded with osteoblasts; to allow vascularization, this portion of the scaffolds must provide the space for vessel ingrowth. Therefore, an interconnected pore network is required. For the portion of the scaffold aimed to regenerate hyaline cartilage, the use of chondrocytes is a natural choice. As cartilage is not vascularized, the structure of the scaffold does not need as large pores as the ones in the bone side. The use of already differentiated cells presents some limitations, since cells must be harvested, expanded in laboratory, seeded in the construct, and finally implanted. Another possibility is the seeding of progenitor cells (Blitterswijk). Since both chondrocytes and osteoblast originates from the bone marrow, the use of bone marrow derived MSCs has attracted significant interest for tissue engineering applications, either when these cells are used alone or in combination with scaffolds (Sundelacruz and Kaplan, 2009; Panseri et al., 2012; Anderson et al., 2014). When MSCs are used, the concept of scaffold design changes, since it must present the right cues to direct their differentiation toward the osteogenic and chondrogenic lineage in the proper compartment of the construct. Several studies have aimed at generating scaffolds able to drive MSCs differentiation toward the targeted lineage. Among them, the use of growth factors in soluble form or bound to the scaffold structure are the ones presenting the strongest effects (Singh et al., 2008; Grayson et al., 2010; Budiraharjo et al., 2013). Recent studies demonstrated that MSCs respond to stimuli coming from the matrix stiffness as well (Even-Ram et al., 2006; Tse and Engler, 2011). Cells attaching to a soft material are more prone to differentiate toward the chondrogenic

TABLE 2. *Summary of the Triphasic Scaffolds Described, Indicating the Biomaterials, Cells, and Growth Factors used and the Main Results for Each Construct*

Author	In vitro/in vivo	Material subchondral bone + cells	Intermediate zone material + cells	Material cartilage + cells	Main findings
Sherwood et al., 2002	In vitro	L-PLGA (85:15)/TCP with 55% porosity	Increment in porosity and PLLA content	Salt leached D,L-PLGA (50:50)/L-PLA with 90% porosity + chondrocytes	Composite tensile strenght similar to cancellous bone, cartilage like tissue
Jiang et al., 2010	In vitro	PLGA microspheres + bioglass seeded with osteoblasts	Chondrocytes embedded in an agarose hydrogel + composite microspheres	Chondrocytes embedded in an agarose hydrogel	Proper tissue in each zone, good stratification
Heymer et al., 2009	In vitro	PLA + HA + βTCP	Hydrophobic phase from the combination of the two phases	Coll I + hyaluronan + hMSCs	Cartilage like cells, coll II, proteoglycans, cartilage specific markers gene
Levingstone et al., 2014	In vitro	Collagen type I and HA + MC3T3	Collagen type I, collagen type II and HA + MC3T3	Collagen type I and II, hyaluronic acid and Na salts + MC3T3	Biocompatibility of the construct
Marquass et al., 2010	In vivo, sheep	TCP	Activated plasma gel	Collagen type I hydrogel	12 months repair comparable to autograft
Liu et al., 2014	In vivo, rabbit	TCP + MSCs		Collagen I and hyaluronan + electrospun PCL mesh + MSCs	Improved regeneration histological scores matched autografts
Dresing et al., 2014	In vivo, rabbit	Salt leached PUR and nano HA	Electrospun PUR	Salt leached PUR	No advantage in tissue healing
Jeon et al., 2014	In vivo, Nude rat/cow	FDM plotted PCL + osteoblasts + rhBMP-7	Electrospun PCL layer + osteoblasts + rhBMP-7	2% Alginate + superficial chondrocyte on the upper part and middle-deep chondrocyte in the lower zone	No cartilage compartimental structure, no bone ingrowth and mineralization

lineage, whereas cells on a stiffer material will be driven toward the osteogenic lineage. Yet, the use of MSCs in the context of classical tissue engineering, where cells are expended and then seeded *in vitro* to allow for tissue formation before constructs can be implanted, presents some limitation, such as the time of culture and the need of external factors for their differentiation *in vitro*. A further approach to overcome this problem may consist of the development of *in vitro* systems that drive the differentiation of MSCs in a regional way, depending on the part of the OC tissue that they will be in contact with. Once such a system is developed and validated with *in vitro* and *in vivo* studies, one could consider to directly implant this scaffold and exploit the intrinsic presence of MSCs in the implantation site. When combined with surgical techniques like microfracture, where small holes are drilled to reach the bone marrow present in the subchondral bone compartment, the bone marrow will flow in the scaffold from the underlying bone providing the MSCs that will colonize the scaffold and differentiate toward the right lineage, depending on the cues provided by the construct.

BIPHASIC CONSTRUCTS

In its most simplistic version, the OC tissue can be seen as a biphasic tissue being composed by a bone phase and a cartilaginous phase. In most studies, biphasic scaffolds are not only based on the different materials or structures of the two components, but also on the different cells cultured in the resulting scaffolds. In 2000, the work of Schaefer et al. presented an *in vitro* engineered scaffold based on PGA nonwoven meshes seeded with primary bovine chondrocytes and PLGA/PEG foams seeded with expanded periosteal cells. The two constructs showed promising results *in vitro*, due to an increase in GAG production in the cartilage side, an increase in mineralization of the ECM in the bone side, and a good integration of the two phases after 4 weeks of culture (Schaefer! et al., 2000). Similarly, in the work of Schek et al. (2004) the constructs presented a biphasic design in material, cell types, and growth factors. The scaffold consisted of the combination of HA-based ceramic on the bone side and a PLLA sponge on the cartilage side. The two parts were seeded with fibroblasts expressing BMP-7 on the ceramic side and chondrocytes within the sponge. The implantation of these constructs in nude mice determined the generation of a biphasic tissue with all the structures present in the OC interface, bone and blood vessel in the ceramic part, a mineralized transition tissue, and a cartilaginous tissue on the polymeric side.

These examples showed initial promising results in achieving OC tissue regeneration. Yet, the scaffold structures developed in these studies are still characterized by a tortuous and not completely interconnected pore network, thus limiting their potential translation to larger defects, where nutrient diffusion and waste removal become more critical for the viability and functionality of the regenerated tissue. For these reasons, additive manufacturing technologies gathered a great interest and momentum in the past two decades, due to their versatility in tuning scaffold features such as fiber spacing, fiber diameter and fiber deposition pattern. This allows one to obtain fully interconnected 3D structures with customizable pore network, resulting in a high flexibility in tuning physicochemical, structural, and mechanical properties of the fabricated scaffolds. Cao et al. (2003) studied the coculture of iliac crest stromal cells and chondrocyte in a biphasic PCL construct. The scaffold was plotted and then partitioned vertically into two halves with a gap between them, leaving only a small portion in contact with each other. The first half was seeded with iliac crest stromal cells and cultured for 18 days under osteogenic conditions, and the other half was seeded with rib cartilage chondrocytes. The resulting coculture construct was cultured *in vitro* for 8 weeks in a coculture medium. The two compartments were kept together by the addition of fibrin glue to both cell suspensions prior to seeding. Even though the *in vitro* results were satisfactory, additional analysis before further use of this scaffold *in vivo* should be performed, as also suggested by the authors. More recently, Ding et al. (2013) tested a biphasic scaffold to regenerate a goat femoral head. This *in vivo* study was carried out in nude mice, and the results were analyzed by using goat proximal femoral condyles as positive controls and implanted cell-free scaffolds as negative controls. The scaffold had a femoral condyle shape and consisted of a lower part made of a blend of PCL and HA plotted via fused deposition modeling, on top of which a nonwoven fiber scaffolds of PGA/PLA was located to regenerate the articular cartilage tissue of the femoral head. The two components of the scaffolds were seeded with goat hMSCs in the bone compartment and chondrocytes in the cartilage compartment, respectively. The cell seeded constructs were combined after 2–3 weeks of culture under osteogenic medium for the lower part and chondrogenic medium for the top part. The combined scaffolds were implanted and analyzed after 10 weeks, showing expression of osteogenic and chondrogenic markers in the two components, whereas the negative controls presented only sparse fibrotic tissue. Furthermore, this system generated an interface zone, in which hypertrophic cartilage with immature calcified tissue could be observed, thus approaching the structural and biophysical properties of the native tissue.

To test scaffolds for OC regeneration *in vivo* the use of mice or rats is limiting, allowing only subcutaneous implantations. Larger animal models, such as rabbits, pigs, or goats, are necessary to fully validate new scaffolds in an orthotopic implantation model. Kandel et al. (2006) produced a porous calcium polyphosphate (CPP) scaffold seeded with autologous chondrocytes and implanted the construct in a sheep OC defect. The scaffolds supported OC regeneration with shown indications of cartilage

maturation, bone ingrowth, and fusion, proceeding from 4 to 9 months of implantation. Yet, some fibrotic tissue was also observed at the bone interface, thus indicating a suboptimal integration of the construct. Duan et al. (2013) tested biphasic scaffolds with different pore sizes in combination with and without MSCs in a rabbit model for OC regeneration. The scaffolds were prepared by PLGA salt leaching technique and presented a top part for the chondral regeneration with height of 1 mm and an osseous layer of 4 mm. The constructs were implanted for 12 weeks. The scaffolds without cells displayed better results than the untreated defects, although the defects implanted with cell-free scaffolds showed inferior repair in the chondral layer. Among the 5 pore sizes combinations tested, the construct with the best histological and biochemical scores had pore size of 100–200 μm for the chondral side, and 300–450 for the osseous part in combination with cells.

The use of already differentiated autologous cells has some limitations in terms of source and harvesting procedures. Thus, to overcome these drawbacks and to mimic what happens in the healing process of bone and cartilage, research efforts moved to the use of MSCs. To direct their differentiation toward the chondrogenic and the osteogenic lineage, the design of scaffolds geared to further functionalization to present growth factors in the right construct location in space and time. The combination of MSC seeded scaffolds and delivery of biological signals was studied *in vivo* by Chen et al. (2011). The constructs consisted of a plasmid TGF-β1-activated chitosan-gelatin scaffold for the chondrogenic layer and a plasmid BMP-2-activated HA/chitosan-gelatin scaffold for the osteogenic layer. The structures were separately seeded with human MSCs and cultured for 1 week. Prior to implantation, the separated constructs were fused with fibrin glue and cultured for another week *in vitro*. The constructs promoted the growth and differentiation of MSCs and supported the regeneration of articular cartilage and subchondral bone in a rabbit knee defect after 12 weeks of implantation. The same outcome was reached one year later by Re'em et al. (2012), with a cell-free scaffold based on 0.1% alginate-sulfate (w/v), 1% alginate (w/v), and 0.18% (w/v) D-gluconic acid/hemicalcium salt loaded with TGF-β1 and BMP-4 prepared *in situ*. After 4 weeks of implantation in rabbits, the top layer was integrated with the surrounding cartilage and displayed the typical ECM composition of hyaline cartilage with no signs of mineralization. The bottom part presented newly formed woven bone.

The use of biphasic scaffolds has shown some degree of success, therefore highlighting that the strategy to mimic, as closely as possible the native OC tissue is a promising route for functional regeneration. However, when strictly looking at biomimicry principles, biphasic scaffolds are not satisfactory, since they treat bone and cartilage as two distinct compartments, whereas the two tissues are intimately interconnected, as previously explained. Additionally, in most of the above presented studies the presence of only two parts implicitly neglected the presence of the transition zone of calcified cartilage. Furthermore, biphasic scaffolds do not display all the gradients that characterize the OC tissue and the further division of cartilage into its specific zones.

TRIPHASIC AND MULTILAYERED SCAFFOLDS

In an effort to mimic more closely the native OC tissue, triphasic, or multilayered scaffolds have been developed by several groups. Two studies presented an intriguing scaffold design but their biological relevance was not studied *in vitro* nor *in vivo* (Harley et al., 2010; Aydin, 2011). In the first case, a gradient in mechanical properties was generated. In the second study, only natural materials from the OC ECM were used and an interface similar in ECM properties to the natural OC tissue interface was generated via the phenomena of interdiffusion of the two material phases followed by freeze drying. The bone side of the triphasic scaffolds is the most consistent since the major part of the studies found in literature presented a composite of PLGA or PLA combined with tricalcium phosphate, bioglasses or HA. However, the cartilaginous portion varied in composition, material used, and production method. In 2002, Sherwood et al. (2002) presented multiphasic scaffolds. Each phase consisted of a different porosity, material composition and stiffness. The cartilage compartment was made with D,L-PLGA (50:50)/L-PLA with 90% porosity obtained by salt leaching. The bone compartment was a composite made with L-PLGA (85:15)/tricalcium phosphate with a porosity of 55%. To prevent delamination, the intermediate area presented an increase in porosity (from 65 to 85%) as well as in lactic acid content (from PLGA 85:15 to PLGA 50:50 PLA), when moving from the bone to the cartilage compartment. The mechanical testing proved that the composite had a tensile strength similar to cancellous bone. Chondrocytes were seeded, preferably attached to the cartilage scaffold compartment, and after 6 weeks of culture *in vitro* formed cartilage like tissue. By solving the problem of delamination, however, the resemblance of the construct to OC tissue was compromised. A better result in terms of tissue stratification within the construct was obtained by Jiang et al. (2010). In this study, the variation in phases was generated by different combinations of materials and cells. Similarly, to the work of Sherwood, the bone compartment was based on PLGA microspheres with a mineral part consisting of bioglass seeded with osteoblasts. Chondrocytes embedded in an agarose hydrogel formed the cartilage compartment. The intermediate phase was similar to the cartilage one, with the addition of PLGA and bioglass ceramic microspheres, in order to stimulate the formation of mineralized cartilage. In each region, cells formed the proper tissue. Even if in the intermediate zone no markers of hypertrophic

cartilage were analyzed, chondrocyte within a mineralized matrix were observed. The stratification of tissues within the construct was satisfactory. However, hydrogels lack sufficient mechanical properties, which are in the order of magnitude of 10–100 kPa, whereas cartilage and subchondral bone mechanical properties are in the order of 0.45–0.8 MPa (Mansour) and 2.3 ± 1.5 GPa (Mente and Lewis, 1994), respectively. Beside the similarities in the bone compartment, Heymer et al. (2009) used a different approach for the design of the chondral side. A porous layer of 3 mm of bovine collagen type I and hyaluronan comprised the cartilage portion, while the bone side was based on PLA composite with a mineral phase of HA and β-tricalcium phosphate. In between the two layers, a hydrophobic region resulted from joining the two structures. The study focused on cartilage regeneration only. Human MSCs were suspended in a collagen type I gel and seeded on the upper layer. After 3 weeks of culture under chondrogenic conditions, chondrocyte-like cells were visible in the upper third of the top layer and were surrounded by collagen type II and proteoglycans. At a molecular level, cells expressed specific marker genes such as COMP, aggrecan, and collagen types II and X. Despite promising results for cartilage regeneration, the lack of bone regeneration results in only a partial validation of such a scaffold design. Recently, Levingston et al. (2014) developed a system to generate gradients in material composition, stiffness, and porosity via an "iterative layering" freeze-drying technique, based on the consequent apposition of layers on top of each other followed by freeze-drying. This design differed from the previous one as the scaffold composition was based only on natural polymers commonly found in the OC ECM. The bone layer was comprised of a commercial form of collagen type I and HA. The intermediate layer consisted of a mixture of collagen types I and II, and HA. Similarly, the cartilaginous layer was based on collagen types I and II, HA, and sodium salts. The scaffolds were seeded with MC-3T3 pre-osteoblasts, which proliferated and populated all the compartments over a period of 14 days confirming the biocompatibility of the construct. Such constructs may be promising for OC applications, although an *in vitro* study with human cells and validation in preclinical animal models are needed to further confirm these preliminary results.

Three-layered constructs were also tested in vivo in large animal models. In 2010, Marquass et al. (2010) compared OC autografts with scaffolds presenting a collagen type I hydrogel on the chondral side, an intermediate activated plasma gel phase and a tricalcium phosphate osseous phase. The constructs were seeded with pre-differentiated autologous MSCs toward the chondrogenic lineage and implanted for 6 and 12 months in an OC defect in sheep knee. No major differences in terms of histological scores were displayed by the groups. At 12 months, biomechanical and macroscopic analysis did not show any difference. Autologous MSC-seeded triphasic implants showed comparable repair quality to OC autografts in terms of histology and biomechanical testing. More recently, multilayered scaffolds based on synthetic polymers, such as PCL and polyurethane, with and without the addition of natural ECM components, were evaluated in vivo by Liu et al. (2014) and by Dresing et al. (2014). In both studies, MSCs were seeded and the scaffolds implanted in a rabbit model for 12 weeks. Starting from an electrospun PCL mesh as periosteal scaffold, Liu et al. freeze-dried it first with a collagen type I and hyaluronan solution, in order to generate the cartilage portion, and then with tricalcium phosphate for the osseous phase. The electrospun mesh promoted the alignment of seeded bone marrow derived MSCs seeded in a fashion resembling the superficial zone of hyaline cartilage. The cell-seeded triphasic construct led to an improved regeneration of an OC defect in a rabbit model matching the histological scores of autografts (Liu et al., 2014). The fully synthetic construct used by Dresing et al.(2014) was based on poly(ester-urethane) (PUR) in different structures for the regeneration of cartilage, subchondral bone, and cortical bone. The cartilage compartment was made by salt leached PUR, the subchondral bone compartment by electrospun PUR, and the bone compartment by a salt leached combination of PUR and nano HA. The bone and cartilage side presented a similar porosity, 85% and 87%, respectively. The major differences were found in terms of average pore size 121 and 251 μm, respectively, and of the addition of the mineral phase, resulting in a stiffness of 0.98 N/mm for the PUR scaffold alone and of 2.18 N/mm for the composite PUR. Despite the elastomeric PUR was easily press fitted in the OC defect, it did not provide any advantage for tissue healing after 12 weeks. Furthermore, this construct could not be really considered as a gradient structure, since the intermediate phase could not be compared with the other two. Additionally, this marked difference between the subchondral bone and the calcified cartilage does not resemble the anatomical transition, in which the two compartment are highly interdigitated (Ferguson et al., 2003). More recently, Jeon et al. (2014) developed a system to study OC development ectopically in a nude rat. The desired scaffold to be tested was fitted into a cylindrical shaped bovine OC plugs, and then implanted subcutaneously in rats. This novel system may allow a higher throughput screening of several OC constructs at the same time than conventional subcutaneous implantation, accounting for the possibility to test up to 8 constructs per animal, thus reducing the number of animals used and associated costs In this study, a multiphasic scaffold was tested, based on bilayered 2% alginate containing superficial chondrocyte on the upper part and middle-deep chondrocyte in the lower zone for the cartilage compartment, which was joined with a PCL fused deposition

modeling scaffold on top of an electrospun PCL layer, both seeded with osteoblasts, for the bone and interface compartments. Immediately before implantation, the bone compartment was also loaded with rh-BMP7. After 12 weeks, the scaffolds were analyzed. The use of bilayered cartilage gel, however, did not recapitulate the compartmental structure of the native cartilage, nor zone specific GAG distribution. Likewise, the bone compartment lacked bone ingrowth and mineralization, probably due to insufficient vascularization. Despite the negative results obtained, this study presented an elegant and new method for screening several OC constructs. The division of the scaffold in several zones aimed at resembling the gradient behavior of the OC interface. Yet, one of the main possible limitations in this study was the size of the construct, a 7 mm long scaffold, which might have encountered some difficulties in integrating with the surrounding tissue, likely due to the lack of associated vasculature.

CONTINUOUS GRADIENT SCAFFOLDS

In several studies, the Detamore's group proposed and tested an effective method to overcome the limitation encountered in the production of discrete gradient scaffolds (Singh et al., 2008, 2010; Dormer et al., 2010, 2011; Mohan et al., 2011, 2014). The first step consisted of the generation of poly(D,L-lactide-*co*-glycolide) (PLGA) microspheres, in which a desired compound can be added (Singh et al., 2008). The loaded microspheres were dispersed in distilled water/PVA solution and placed in two syringes each connected to a pump to control the flow. The suspension was then pumped into a cylindrical mold by varying the flow, in order to generate an opposite gradient. The water/PVA was pumped out and the particles were soaked in ethanol to facilitate physical attachment among adjacent microspheres. An additional freeze-drying step was then performed. The microspheres were loaded with $CaCO_3$ and TiO_2 (Singh et al., 2010), TGF-β1 and BMP-2 (Dormer et al., 2010), and chondroitin-sulfate and bioglass (Mohan et al., 2014). If a single gradient was desired, one pump was loaded with pure PLGA microspheres. The biocompatibility of the system was tested on porcine chondrocytes (Singh et al., 2008) and human umbilical cord MSCs (Singh et al., 2010). When the microspheres were loaded with bioactive signals, cells seeded on gradient scaffolds outperformed the controls after 6 weeks of culture in terms of cell number, protein content, and gene expression of osteogenic and chondrogenic markers (Dormer et al., 2010). After these promising results in vitro, scaffolds based on microspheres loaded with BMP-2 on the bone side and TGF-β1 on the cartilage side were implanted in a small mandibular condyle rabbit model (Dormer et al., 2011). The profile for gradient constructs was linear, such that the transition region from TGF-β1 to BMP-2 comprised the second quarter of the scaffold volume, while the top quarter and bottom half contained all TGF-β1 or BMP-2-loaded microspheres, respectively. After 6 weeks of implantation, histological and MRI analysis proved the addition of bioactive signals to be less effective than expected. On the cartilage side, the mechanical support of the scaffold played a more predominant role than the presence of TGF-β1 in generating a smoother and thicker cartilage layer, when compared with the nontreated defect. BMP-2 led to thicker trabeculae, but also on this side, the mechanical support of the scaffold played a greater role, since the subchondral bone layer was more uniform in the gradient and blank scaffolds compared with the nontreated ones. The total bone apposition was not greatly influenced either, probably due to the small size of the defect. An evolution of this system was presented in 2013. The PLGA microspheres were loaded with bioactive signals in combination with components of the ECM. The region of the scaffold designed for osteogenic differentiation presented microspheres loaded with BMP-2 and bioglass, decreasing in number toward the other side of the scaffold, rich in microspheres loaded with TGF-β3 and chondroitin sulfate. MSCs displayed a higher deposition of ECM markers when seeded on scaffolds loaded with the raw material, in comparison to scaffolds presenting the growth factors alone. Cells seeded in scaffolds containing opposing gradients of CS/TGF-β3 and BG/BMP-2 produced clear regional variations in the secretion of tissue-specific ECM. Overall, this microsphere-based scaffold proved to be an effective way to incorporate different biological signals of various natures in a scaffold and generate opposite gradients of more than one compound, thus closing the gap, to mimic the gradient behavior of the OC tissue.

Most of the relevant studies connected to the use of gradient scaffolds for the treatment of OC defects have involved the use of scaffolds presenting discrete gradients only. Although the OC interface presents discrete variations when moving from the subchondral bone to the cartilaginous compartment, a continuous gradient is present within hyaline cartilage. A combinatorial approach of the multilayered technique and the solution proposed by Detamore's group can find, therefore, a possible application in the development of a scaffold resembling even more the characteristics of the OC interface.

THE GRADIENT IN THE CLINICS

Currently, only three gradient scaffold designs reached the phase of clinical trials (Fig. 4). Two of them are biphasic scaffolds and the last one is a triphasic scaffold design. TruFi™ (Smith and Nephew, Andover, MA) is a biphasic scaffold based on PLGA-PGA 75:25 and calcium phosphate, which are glued together with a small amount of solvent after preparation. The cartilage phase was prepared by the addition of 10% poly(glycolide), reinforcing fibers to a blend of PLGA-PGA 75:25 to improve the compressive modulus (Slivka et al., 2001). The addition of the bone

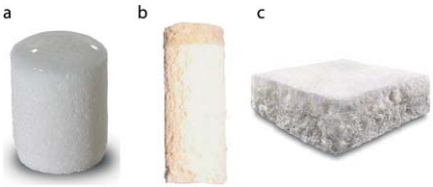

FIGURE 4. *Pictures of the scaffolds which reached the clinical trials, a) Aragonite-based osteochondral scaffold (Agili-C™, CartiHeal (2009) Ltd, Israel), b) polimeric PLGA-PGA and Calciun sulfate bi-layer scaffold (Trufit CB™, Smith & Nephew, USA) and c) HA-Collagene type I three-layer scaffold (Maioregen™, Finceramica, Italy). Modified from Elizaveta Kon, 2014.*

compartment and the effectiveness of the construct in treating an OC defect was assessed in a goat orthotopic model (Niederauer et al., 2000). The 2.7 mm high calcium sulfate cylinder was glued with the previously prepared 1.2 mm high cartilage cylinder, and the glue provided a thin film of 1 mm in thickness at the articulating surface of the implant. Improved healing of the orthotopic defect was shown after 16 weeks from implantation, with abundant hyaline cartilage formation, integration, and good bony restoration. The addition of chondrocyte to the implant was also tested, but did not show any additional beneficial effect. Two clinical studies conducted by Bedi et al. (2010) and Barber and Dockery (2011) showed controversial results. The first study described a slow improvement of the injured site. The second clinical study performed a CT scan on 9 patients with intervals between 2 and 63 months, showing no evidence of bone ingrowth, osteoconductivity, or ossification. The decrease in implant density over time reached levels of fibrous scar. Another study from Quarch et al. (2014) showed no clinical improvement in the 21 patients treated with this scaffold design. After these results, the scaffold was used only to treat cartilage defects. Positive results were obtained by Carmont et al. (2009) on a 18 year old patient with a large chondral defect. The patient returned to sport activities, indicating resolution of pain. Despite these controversial findings, a number of clinical trials were conducted (Dhollander et al., 2012; Joshi et al., 2012; Bekkers et al., 2013; Hindle et al., 2014). In the study of Bekkers et al. (2013), the scaffolds presented newly formed cartilage-like tissue within the implant, which did not damage the opposing and surrounding tissue after 12 months. Other clinical studies showed in the best case modest improvement (Dhollander et al., 2012), but a 70% failure in active patients in the worst cases (Joshi et al., 2012). From these studies, a general slow healing process with controversial end results provided by the TruFit™ plug have been observed, thus justifying for the continuous research for more functional scaffold designs.

Another biphasic scaffold, which reached the clinical practice, was developed by Kon et al. (2009). The design was based on calcium carbonate in the form of crystalline aragonite for the bone side and on hyaluronic acid for the cartilage compartment (Kon et al., 2014a,2014b,2014c,2014d). The first study performed in a goat model aimed at defining the best construct design. The impregnation with hyaluronic acids and the presence of drilled channels were tested. A defect of 6 mm in diameter and 8 mm deep was made in the medial femoral condyle and the scaffolds were implanted for 6 months. Scaffolds presenting two drilled phases outscored the other groups by displaying a smooth contour and newly formed hyaline cartilage, well integrated with the surrounding native cartilage, and with subchondral bone, respectively. This construct hits the clinic in a first-in-man experiment. It was used in a 47 years old nonprofessional sportsman, resulting in successful treatment of a post traumatic femoral condyle lesion of 2 cm^2. After 18 months, the man returned to his preinjury sport activity. MRI analysis at 24 months follow-up showed promising results in terms of restoration of the articular cartilage (Kon et al., 2014a,2014b,2014c,2014d).

Among the multilayered scaffolds for OC regeneration, a biomimetic construct consisted of different compositions for each zone was also developed by Kon et al. (2009). The cartilage compartment was based on pure collagen type I, a tidemark-like structure was obtained by combining collagen type I and HA in a 60:40 weight ratio, and a mineralized portion corresponding to the subchondral bone presented a 30:70 weight ratio composition of collagen type I and HA (Fin-Ceramica, Faenza, Italy). The three components were synthesized separately and combined together on top of a Mylar sheet, freeze dried, and gamma sterilized. The intermediate and lower layers were formed by nucleating bone-like nanostructured nonstoichiometric HA into self-assembling collagen fiber, reproducing what happens at the biological level in the neo-ossification process. The resulting construct presented a gradient in mineral content from the bone to the chondral side and a gradient in collagen content in the opposite direction. The first study was performed in a horse animal model, testing the efficacy of bilayered and trilayered scaffolds for the regeneration of chondral and OC lesions (Kon et al., 2010a, 2010b). The trilayered scaffolds were produced as mentioned above, whereas the bilayered scaffolds were missing the lower part, since they were intended for the regeneration of a chondral damage. After 6 weeks of implantation, both the chondral and OC lesions were filled. The newly formed trabecular bone was visible at the subchondral level and a tide mark-like region was present. Unfortunately, fibrocartilage and not hyaline cartilage filled the chondral compartment and a first alignment of the collagen fibers was observed. In a subsequent study, the addition of autologous chondrocytes seeded within the trilayered scaffold was studied in a sheep orthotopic model to assess any additional beneficial effect of cells (Kon et al., 2009). After a 6 months implantation, the presence of newly formed cartilage in contact with the surrounding tissue was observed in the constructs with and without

cells. In the lower compartment, newly formed subchondral bone was observed. The presence within the subchondral compartment of collagen type II and cells with hypertrophic chondrocyte morphology suggested that the scaffold-mediated regeneration of subchondral bone followed an endochondral ossification process.

The use of the previously described biomimetic graded scaffolds were applied in a clinical study for the repair of knee chondral or OC lesion. An early analysis on its stability was carried out in a pilot clinical trial. The first study confirmed the attachment of the graft and only a partial detachment in 2 patients out of 15. Visual scoring of the repaired tissue revealed a normal repair score in one case and a near-normal repair score in the other cases. Subchondral bone formation without the presence of biomaterial was showed by histological analysis, thus indicating the possible complete resorption of the biomaterial after 6 months. The cartilage tissue appeared not only repaired but engaged in an ongoing maturation process (Kon et al., 2010a,2010b). These encouraging results led to a longer follow-up with randomized studies. A cluster of 27 patients were followed for 2 and 5 years after surgery for knee chondral or OC lesions (size 1.5–6 cm^2; Kon et al., 2014a,2014b,2014c,2014d). Results showed a significant increase of the quality of the regenerated tissue following the International Knee Documentation Committee subjective score. The individual's activity level, measured by Tenger scores, depicted an increase from the preoperatory to the 2 and 5 years follow-up. The Tenger scores remained lower than the one before the injury, but did not reach a statistically significant difference. After 2 years the cartilage resulted completely filled in 65.2% of the treated cases, the construct was completely integrated in 69.6% of the cases, intact repair tissue surface was observed in 56.5% of the cases, and a homogeneous structure of the repair tissue in 34.8% of the patients. However, the subchondral lamina and bone resulted intact in only 7 and 47% of the cases, respectively (Kon et al., 2011). At 5 years follow-up, MRI evaluation revealed a significant improvement in both cartilage and subchondral bone status.

CONCLUSIONS

In this review, the gradients governing the regeneration of the OC interface were presented alongside an overview of the solution from the laboratory bench to the bed side. The OC tissue is based on gradients from the early developmental stage until the fully developed body in the adult organism. Nowadays, a lot of effort is made to design scaffolds that lead to the healing of the OC interface, attempting to re-establish the gradient present in the patient. We have presented a few promising methods for the regeneration of the OC tissue. To overcome the abnormalities that still persist after midterm follow-up in clinical trials so far available, a colloaboration between material scientists, clinicians, and developmental biologists should be sought, to elucidate those mechanisms and pathways involved in the early stage of bone and cartilage development, and include those signals into structures able to trigger not only healing of the tissue, but also a proper regeneration.

REFERENCES

Anderson JA, Little D, Toth AP, Moorman CT, Tucker BS, Ciccotti MG, Guilak F. 2014. Stem cell therapies for knee cartilage repair: the current status of preclinical and clinical studies. Am J Sports Med 42:2253–2261.

Aydin HM. 2011. A Three-layered osteochondral plug: structural, mechanical, and in vitro biocompatibility analysis. Adv Eng Mater 13:B511–B517.

Barber FA, Dockery WD. 2011. A computed tomography scan assessment of synthetic multiphase polymer scaffolds used for osteochondral defect repair. Arthroscopy 27:60–64.

Bedi A, Foo LF, Williams RJ, Potter HG, Group TCS. 2010. The maturation of synthetic scaffolds for osteochondral donor sites of the knee: an MRI and T2-mapping analysis. Cartilage 1:20–28.

Bekkers JE, Bartels LW, Vincken KL, Dhert WJ, Creemers LB, Saris DB. 2013. Articular cartilage evaluation after TruFit plug implantation analyzed by delayed gadolinium-enhanced MRI of cartilage (dGEMRIC). Am J Sports Med 41:1290–1295.

Benders KE, van Weeren PR, Badylak SF, Saris DB, Dhert WJ, Malda J. 2013. Extracellular matrix scaffolds for cartilage and bone regeneration. Trends Biotechnol 31:169–176.

Bhosale AM, Richardson JB. 2008. Articular cartilage: structure, injuries and review of management. Br Med Bull 87:77–95.

Bianco P, Cancedda FD, Riminucci M, Cancedda R. 1998. Bone formation via cartilage models: the "borderline" chondrocyte. Matrix Biol 17:185–192.

Blitterswijk CV. Tissue Engineering. Clemens van Blitterswijk, Peter Thomsen, Anders Lindahl, Jeffrey Hubbell, David F. Williams, Ranieri Cancedda, Joost D. de Bruijn and Jérôme Sohier, editors. ISBN: 978-0-12-370869-4

Bobinac D, Spanjol J, Zoricic S, Maric I. 2003. Changes in articular cartilage and subchondral bone histomorphometry in osteoarthritic knee joints in humans. Bone 32:284–290.

Buckwalter JA, Mow VC, Ratcliffe A. 1994. Restoration of injured or degenerated articular cartilage. J Am Acad Orthop Surg 2: 192–201.

Budiraharjo R, Neoh KG, Kang ET. 2013. Enhancing bioactivity of chitosan film for osteogenesis and wound healing by covalent immobilization of BMP-2 or FGF-2. J Biomater Sci Polym Ed 24: 645–662.

Cao T, Ho KH, Teoh SH. 2003. Scaffold design and in vitro study of osteochondral coculture in a three-dimensional porous

polycaprolactone scaffold fabricated by fused deposition modeling. Tissue Eng 9:S103–S112.

Carmont MR, Carey-Smith R, Saithna A, Dhillon M, Thompson P, Spalding T. 2009. Delayed incorporation of a TruFit plug: perseverance is recommended. Arthroscopy 25:810–814.

Chen G, Deng C, Li YP. 2012. TGF-β and BMP signaling in osteoblast differentiation and bone formation. Int J Biol Sci 8:272–288.

Chen J, Chen H, Li P, Diao H, Zhu S, Dong L, Wang R, Guo T, Zhao J, Zhang J. 2011. Simultaneous regeneration of articular cartilage and subchondral bone in vivo using MSCs induced by a spatially controlled gene delivery system in bilayered integrated scaffolds. Biomaterials 32:4793–4805.

Chimal-Monroy J, Diaz de LL. 1999. Expression of N-cadherin, N-CAM, fibronectin and tenascin is stimulated by TGF-beta1, beta2, beta3 and beta5 during the formation of precartilage condensations. Int J Dev Biol 43:59–67.

Dawson J, Linsell L, Zondervan K, Rose P, Randall T, Carr A, Fitzpatrick R. 2004. Epidemiology of hip and knee pain and its impact on overall health status in older adults. Rheumatology (Oxford) 43:497–504.

de Crombrugghe B, Lefebvre V, Nakashima K. 2001. Regulatory mechanisms in the pathways of cartilage and bone formation. Curr Opin Cell Biol 13:721–728.

Dhollander AA, Liekens K, Almqvist KF, Verdonk R, Lambrecht S, Elewaut D, Verbruggen G, Verdonk PC. 2012. A pilot study of the use of an osteochondral scaffold plug for cartilage repair in the knee and how to deal with early clinical failures. Arthroscopy 28:225–233.

Ding C, Qiao Z, Jiang W, Li H, Wei J, Zhou G, Dai K. 2013. Regeneration of a goat femoral head using a tissue-specific, biphasic scaffold fabricated with CAD/CAM technology. Biomaterials 34: 6706–6716.

Dormer NH, Busaidy K, Berkland CJ, Detamore MS. 2011. Osteochondral interface regeneration of rabbit mandibular condyle with bioactive signal gradients. J Oral Maxillofac Surg 69:e50–e57.

Dormer NH, Singh M, Wang L, Berkland CJ, Detamore MS. 2010. Osteochondral interface tissue engineering using macroscopic gradients of bioactive signals. Ann Biomed Eng 38:2167–2182.

Dresing I, Zeiter S, Auer J, Alini M, Eglin D. 2014. Evaluation of a press-fit osteochondral poly(ester-urethane) scaffold in a rabbit defect model. J Mater Sci Mater Med 25:1691–1700.

Duan P, Pan Z, Cao L, He Y, Wang H, Qu Z, Dong J, Ding J. In press. The effects of pore size in bilayered poly(lactide-co-glycolide) scaffolds on restoring osteochondral defects in rabbits. J Biomed Mater Res A.

Dunlop DD, Manheim LM, Song J, Chang RW. 2001. Arthritis prevalence and activity limitations in older adults. Arthritis Rheum 44:212–221.

Durr J, Lammi P, Goodman SL, Aigner T, von der Mark K. 1996. Identification and immunolocalization of laminin in cartilage. Exp Cell Res 222:225–233.

Even-Ram S, Artym V, Yamada KM. 2006. Matrix control of stem cell fate. Cell 126:645–647.

Falchuk KH, Goetzl EJ, Kulka JP. 1970. Respiratory gases of synovial fluids: an approach to synovial tissue circulatory-metabolic imbalance in Rheumatoid Arthritis. Am J Med 49:223–231.

Farnum CE, Lee R, O'Hara K, Urban JPG. 2002. Volume increase in growth plate chondrocytes during hypertrophy: the contribution of organic osmolytes. Bone 30:574–581.

Ferguson VL, Bushby AJ, Boyde A. 2003. Nanomechanical properties and mineral concentration in articular calcified cartilage and subchondral bone. J Anat 203:191–202.

Fermor B, Christensen SE, Youn I, Cernanec JM, Davies CM, Weinberg JB. 2007. Oxygen, nitric oxide and articular cartilage. Eur Cell Mater 13:56–65; discussion 65.

Furumatsu T, Tsuda M, Taniguchi N, Tajima Y, Asahara H. 2005. Smad3 induces chondrogenesis through the activation of SOX9 via CREB-binding protein/p300 recruitment. J Biol Chem 280: 8343–8350.

Gamer LW, Ho V, Cox K, Rosen V. 2008. Expression and function of BMP3 During chick limb development. Dev Dyn 237:1691–1698.

Glant TT, Hadhazy C, Mikecz K, Sipos A. 1985. Appearance and persistence of fibronectin in cartilage. Specific interaction of fibronectin with collagen type II. Histochemistry 82:149–158.

Goldring MB, Tsuchimochi K, Ijiri K. 2006. The control of chondrogenesis. J Cell Biochem 97:33–44.

Grayson WL, Bhumiratana S, Grace Chao PH, Hung CT, Vunjak-Novakovic G. 2010. Spatial regulation of human mesenchymal stem cell differentiation in engineered osteochondral constructs: effects of pre-differentiation, soluble factors and medium perfusion. Osteoarthritis Cartilage 18:714–723.

Harada S, Rodan GA. 2003. Control of osteoblast function and regulation of bone mass. Nature 423:349–355.

Harley, BA, Lynn, AK, Wissner-Gross, Z, Bonfield, W, Yannas IV, Gibson LJ. 2010. Design of a multiphase osteochondral scaffold III: fabrication of layered scaffolds with continuous interfaces. J Biomed Mater Res Part A 92A:1078–1093.

Hayes AJ, MacPherson S, Morrison H, Dowthwaite G, Archer CW. 2001. The development of articular cartilage: evidence for an appositional growth mechanism. Anat Embryol (Berl) 203:469–479.

Heinegard D, Oldberg A. 1989. Structure and biology of cartilage and bone matrix noncollagenous macromolecules. FASEB J 3: 2042–2051.

Heldin CH, Miyazono K, ten Dijke P. 1997. TGF-beta signalling from cell membrane to nucleus through SMAD proteins. Nature 390:465–471.

Heymer A, Bradica G, Eulert J, Nöth U. 2009. Multiphasic collagen fibre–PLA composites seeded with human mesenchymal stem cells for osteochondral defect repair: an in vitro study. J Tissue Eng Regen Med 3:389–397.

Hindle P, Hendry JL, Keating JF, Biant LC. 2014. Autologous osteochondral mosaicplasty or TruFit plugs for cartilage repair. Knee Surg Sports Traumatol Arthrosc 22:1235–1240.

Hunziker EB. 2002. Articular cartilage repair: basic science and clinical progress. A review of the current status and prospects. Osteoarthritis Cartilage 10:432–463.

Hunziker EB, Quinn TM, Hauselmann HJ. 2002. Quantitative structural organization of normal adult human articular cartilage. Osteoarthritis Cartilage 10:564–572.

Itoh F, Asao H, Sugamura K, Heldin CH, ten Dijke P, Itoh S. 2001. Promoting bone morphogenetic protein signaling through negative regulation of inhibitory smads. EMBO J 20:4132–4142.

Jeon JE, Vaquette C, Theodoropoulos C, Klein TJ, Hutmacher DW. 2014. Multiphasic construct studied in an ectopic osteochondral defect model. J R Soc Interface 11:20140184.

Jiang J, Tang A, Ateshian G, Guo XE, Hung C, Lu H. 2010. Bioactive stratified polymer Ceramic-hydrogel scaffold for integrative osteochondral repair. Ann Biomed Eng 38:2183–2196.

Joshi N, Reverte-Vinaixa M, Diaz-Ferreiro EW, Dominguez-Oronoz R. 2012. Synthetic resorbable scaffolds for the treatment of isolated patellofemoral cartilage defects in young patients: magnetic resonance imaging and clinical evaluation. Am J Sports Med 40: 1289–1295.

Kandel RA, Grynpas M, Pilliar R, Lee J, Wang J, Waldman S, Zalzal P, Hurtig M. 2006. Repair of osteochondral defects with biphasic cartilage-calcium polyphosphate constructs in a sheep model. Biomaterials 27:4120–4131.

Kawano Y, Kypta R. 2003. Secreted antagonists of the wnt signalling pathway. J Cell Sci 116:2627–2634.

Knothe Tate ML, Adamson JR, Tami AE, Bauer TW. 2004. The osteocyte. Int J Biochem Cell Biol 36:1–8.

Kobayashi T, Chung UI, Schipani E, Starbuck M, Karsenty G, Katagiri T, Goad DL, Lanske B, Kronenberg HM. 2002. PTHrP and indian hedgehog control differentiation of growth plate chondrocytes at multiple steps. Development 129:2977–2986.

Komiya Y, Habas R. 2008. wnt signal transduction pathways. Organogenesis 4:68–75.

Kon E, Delcogliano M, Filardo G, Busacca M, Di Martino A, Marcacci M. 2011. Novel nano-composite multilayered biomaterial for osteochondral regeneration: a pilot clinical trial. Am J Sports Med 39:1180–1190.

Kon E, Delcogliano M, Filardo G, Fini M, Giavaresi G, Francioli S, Martin I, Pressato D, Arcangeli E, Quarto R, Sandri M, Marcacci M. 2009. Orderly osteochondral regeneration in a sheep model using a novel nano-composite multilayered biomaterial. J Orthop Res 28:116–124.

Kon E, Delcogliano M, Filardo G, Pressato D, Busacca M, Grigolo B, Desando G, Marcacci M. 2010a. A novel nano-composite multilayered biomaterial for treatment of osteochondral lesions: technique note and an early stability pilot clinical trial. Injury 41: 693–701.

Kon E, Drobnic M, Davidson PA, Levy A, Zaslav KR, Robinson D. 2014a. Chronic posttraumatic cartilage lesion of the knee treated with an acellular osteochondral-regenerating implant: case history with rehabilitation guidelines. J Sport Rehabil 23:270–275.

Kon E, Filardo G, Di Martino A, Busacca M, Moio A, Perdisa F, Marcacci M. 2014b. Clinical results and MRI evolution of a nano-composite multilayered biomaterial for osteochondral regeneration at 5 years. Am J Sports Med 42:158–165.

Kon E, Filardo G, Perdisa F, Venieri G, Marcacci M. 2014c. Clinical results of multilayered biomaterials for osteochondral regeneration. EMBO J 1:10

Kon E, Filardo G, Robinson D, Eisman JA, Levy A, Zaslav K, Shani J, Altschuler N. 2014d. Osteochondral regeneration using a novel aragonite-hyaluronate bi-phasic scaffold in a goat model. Knee Surg Sports Traumatol Arthrosc 22:1452–1464.

Kon E, Mutini A, Arcangeli E, Delcogliano M, Filardo G, Nicoli Aldini N, Pressato D, Quarto R, Zaffagnini S, Marcacci M. 2010b. Novel nanostructured scaffold for osteochondral regeneration: pilot study in horses. J Tissue Eng Regen Med 4:300–308.

Kronenberg HM. 2003. Developmental regulation of the growth plate. Nature 423:332–336.

Kühl M, Sheldahl LC, Park M, Miller JR, Moon RT. 2000. The wnt/Ca2+ pathway: a new vertebrate wnt signaling pathway takes shape. Trends Genet 16:279–283.

Kwan Tat S, Pelletier JP, Amiable N, Boileau C, Lavigne M, Martel-Pelletier J. 2009. Treatment with ephrin B2 positively impacts the abnormal metabolism of human osteoarthritic chondrocytes. Arthritis Res Ther 11:R119.

Leijten JC, Emons J, Sticht C, van Gool S, Decker E, Uitterlinden A, Rappold G, Hofman A, Rivadeneira F, Scherjon S, Wit JM, van Meurs J, van Blitterswijk CA, Karperien M. 2012. Gremlin 1, frizzled-related protein, and Dkk-1 are key regulators of human articular cartilage homeostasis. Arthritis Rheum 64:3302–3312.

Levingstone TJ, Matsiko A, Dickson GR, O'Brien FJ, Gleeson JP. 2014. A biomimetic multi-layered collagen-based scaffold for osteochondral repair. Acta Biomater 10:1996–2004.

Lin AH, Luo J, Mondshein LH, ten Dijke P, Vivien D, Contag CH, Wyss-Coray T. 2005. Global analysis of Smad2/3-dependent TGF-beta signaling in living mice reveals prominent tissue-specific responses to injury. J Immunol 175:547–554.

Liu X, Liu S, Liu S, Cui W. 2014. Evaluation of oriented electrospun fibers for periosteal flap regeneration in biomimetic triphasic osteochondral implant. J Biomed Mater Res B Appl Biomater 102:1407–1414.

Lund-Olesen K. 1970. Oxygen tension in synovial fluids. Arthritis Rheum 13:769–776.

Mannoni A, Briganti MP, Di Bari M, Ferrucci L, Costanzo S, Serni U, Masotti G, Marchionni N. 2003. Epidemiological profile of symptomatic osteoarthritis in older adults: a population based study in dicomano, Italy. Ann Rheum Dis 62:576–578.

Mansour JM. Biomechanics of cartilage. In: Oatis CA, editor. Kinesiology: the mechanics and pathomechanics of human movement. Baltimore, MD: Lippincott Williams & Wilkins; 2003. pp. 1992–1996.

Marquass B, Somerson JS, Hepp P, Aigner T, Schwan S, Bader A, Josten C, Zscharnack M, Schulz RM. 2010. A novel MSC-seeded triphasic construct for the repair of osteochondral defects. J Orthop Res 28:1586–1599.

Martin I, Miot S, Barbero A, Jakob M, Wendt D. 2007. Osteochondral tissue engineering. J Biomech 40:750–765.

Mason RM. 1981. Recent advances in the biochemistry of hyaluronic acid in cartilage. Prog Clin Biol Res 54:87–112.

Mente PL, Lewis JL. 1994. Elastic modulus of calcified cartilage is an order of magnitude less than that of subchondral bone. J Orthop Res 12:637–647.

Miosge N, Flachsbart K, Goetz W, Schultz W, Kresse H, Herken R. 1994. Light and electron microscopical immunohistochemical localization of the small proteoglycan core proteins decorin and biglycan in human knee joint cartilage. Histochem J 26:939–945.

Mohan N, Dormer NH, Caldwell KL, Key VH, Berkland CJ, Detamore MS. 2011. Continuous gradients of material composition and growth factors for effective regeneration of the osteochondral interface. Tissue Eng Part A 17:2845–2855.

Mohan N, Gupta V, Sridharan B, Sutherland A, Detamore MS. 2014. The potential of encapsulating ''raw materials'' in 3D osteochondral gradient scaffolds. Biotechnol Bioeng 111:829–841.

Moroni L, de Wijn JR, van Blitterswijk CA. 2006. 3D fiber-deposited scaffolds for tissue engineering: influence of pores geometry and architecture on dynamic mechanical properties. Biomaterials 27:974–985.

Mundy GR. 2006. Nutritional modulators of bone remodeling during aging. Am J Clin Nutr 83:427S–430S.

Musumeci G, Trovato FM, Loreto C, Leonardi R, Szychlinska MA, Castorina S, Mobasheri A. 2014. Lubricin expression in human osteoarthritic knee meniscus and synovial fluid: a morphological, immunohistochemical and biochemical study. Acta Histochem 116:965–972.

Nakashima K, de Crombrugghe B. 2003. Transcriptional mechanisms in osteoblast differentiation and bone formation. Trends Genet 19:458–466.

Niederauer GG, Slivka MA, Leatherbury NC, Korvick DL, Harroff HH, Ehler WC, Dunn CJ, Kieswetter K. 2000. Evaluation of multiphase implants for repair of focal osteochondral defects in goats. Biomaterials 21:2561–2574.

Nilsson O, Parker EA, Hegde A, Chau M, Barnes KM, Baron J. 2007. Gradients in bone morphogenetic protein-related gene expression across the growth plate. J Endocrinol 193:75–84.

O'Hara BP, Urban JP, Maroudas A. 1990. Influence of cyclic loading on the nutrition of articular cartilage. Ann Rheumc Dis 49: 536–539.

Oegema TR Jr., RJ, Carpenter F, Hofmeister RC, Thompson Jr.. 1997. The interaction of the zone of calcified cartilage and subchondral bone in osteoarthritis. Microsc Res Tech 37:324–332. (). "

Oh SH, Kim TH, Lee JH. 2011. Creating growth factor gradients in three dimensional porous matrix by centrifugation and surface immobilization. Biomaterials 32:8254–8260.

Pacifici M, Golden EB, Oshima O, Shapiro IM, Leboy PS, Adams SL. 1990. Hypertrophic chondrocytes. The terminal stage of differentiation in the chondrogenic cell lineage? Ann N Y Acad Sci 599:45–57.

Panseri S, Russo A, Cunha C, Bondi A, Di Martino A, Patella S, Kon E. 2012. Osteochondral tissue engineering approaches for articular cartilage and subchondral bone regeneration. Knee Surg Sports Traumatol Arthrosc 20:1182–1191.

Pogue R, Lyons K. 2006. BMP signaling in the cartilage growth plate. Curr Top Dev Biol 76:1–48.

Poole CA. 1997. Review. Articular cartilage chondrons: form, function and failure. J Anat 191:1–13.

Poole CA, Flint MH, Beaumont BW. 1984. Morphological and functional interrelationships of articular cartilage matrices. J Anat 138:113–138.

Prydz K, Dalen KT. 2000. Synthesis and sorting of proteoglycans. J Cell Sci 113:193–205.

Quarch VM, Enderle E, Lotz J, Frosch KH. 2014. Fate of large donor site defects in osteochondral transfer procedures in the knee joint with and without TruFit plugs. Arch Orthop Trauma Surg 134:657–666.

Re'em T, Witte F, Willbold E, Ruvinov E, Cohen S. 2012. Simultaneous regeneration of articular cartilage and subchondral bone induced by spatially presented TGF-beta and BMP-4 in a bilayer affinity binding system. Acta Biomater 8:3283–3293.

Rolauffs B, Muehleman C, Li J, Kurz B, Kuettner KE, Frank E, Grodzinsky AJ. 2010. Vulnerability of the superficial zone of immature articular cartilage to compressive injury. Arthritis Rheum 62:3016–3027.

Schaefer! D, Martin I, Shastri P, Padera RF, Langer R, Freed LE, Vunjak-Novakovic G. 2000. In vitro generation of osteochondral composites <1-s2.0-S0142961200001277-main.pdf>." Biomaterials 21:2599–2606.

Schek RM, Taboas JM, Segvich SJ, Hollister SJ, Krebsbach PH. 2004. Engineered osteochondral grafts using biphasic composite solid free-form fabricated scaffolds. Tissue Eng 10:1376–1385.

Sharma A, Jagga S, Lee SS, Nam JS. 2013. Interplay between cartilage and subchondral bone contributing to pathogenesis of osteoarthritis. Int J Mol Sci 14:19805–19830.

Sherwood JK, Riley SL, Palazzolo R, Brown SC, Monkhouse DC, Coates M, Griffith LG, Landeen LK, Ratcliffe A. 2002. A three-dimensional osteochondral composite scaffold for articular cartilage repair. Biomaterials 23:4739–4751.

Shimomura K, Moriguchi Y, Murawski CD, Yoshikawa H, Nakamura N. 2014. Osteochondral tissue engineering with biphasic scaffold: current strategies and techniques. Tissue Eng Part B Rev 20:468–476.

Silver IA. 1975. Measurement of pH and ionic composition of pericellular sites. Philos Trans R Soc Lond B Biol Sci 271:261–272.

Singh M, Berkland C, Detamore MS. 2008. Strategies and applications for incorporating physical and chemical signal gradients in tissue engineering. Tissue Eng Part B Rev. Tissue Eng Part B Rev 14:341–366. doi:10.1089/ten.teb.2008.0304.

Singh M, Dormer N, Salash JR, Christian JM, Moore DS, Berkland C, Detamore MS. 2010. Three-dimensional macroscopic scaffolds with a gradient in stiffness for functional regeneration of interfacial tissues. J Biomed Mater Res A 94:870–876.

Singh M, Morris CP, Ellis RJ, Detamore MS, Berkland C. 2008. Microsphere-based seamless scaffolds containing macroscopic gradients of encapsulated factors for tissue engineering. Tissue EngPart C Methods 14:299–309.

Slivka MA, Leatherbury NC, Kieswetter K, Niederauer GG. 2001. Porous, resorbable, fiber-reinforced scaffolds tailored for articular cartilage repair. Tissue Eng 7:767–780.

Smits P, Dy P, Mitra S, Lefebvre V. 2004. Sox5 and Sox6 are needed to develop and maintain source, columnar, and hypertrophic chondrocytes in the cartilage growth plate. J Cell Biol 164:747–758.

Sobral JM, Caridade SG, Sousa RA, Mano JF, Reis RL. 2011. Three-dimensional plotted scaffolds with controlled pore size gradients: effect of scaffold geometry on mechanical performance and cell seeding efficiency. Acta Biomater 7:1009–1018.

Solchaga LA, Temenoff JS, Gao J, Mikos AG, Caplan AI, Goldberg VM. 2005. Repair of osteochondral defects with hyaluronan- and polyester-based scaffolds. Osteoarthritis Cartilage 13:297–309.

Sundelacruz S, Kaplan DL. 2009. Stem cell- and scaffold-based tissue engineering approaches to osteochondral regenerative medicine. Semin Cell Dev Biol 20:646–655.

Treppo S, Koepp H, Quan EC, Cole AA, Kuettner KE, Grodzinsky AJ. 2000. Comparison of biomechanical and biochemical properties of cartilage from human knee and ankle pairs. J Orthop Res 18:739–748.

Tse JR, Engler AJ. 2011. Stiffness gradients mimicking in vivo tissue variation regulate mesenchymal stem cell fate. PLoS ONE 6: e15978. doi:10.1371/journal.pone.0015978.

Wang Y, Cheng Z, Elalieh HZ, Nakamura E, Nguyen MT, Mackem S, Clemens TL, Bikle DD, Chang W. 2011. IGF-1R signaling in chondrocytes modulates growth plate development by interacting with the PTHrP/ihh pathway. J Bone Miner Res 26:1437–1446.

Woodfield TB, Blitterswijk CAV, Wijn JD, Sims TJ, Hollander AP, Riesle J. 2005. Polymer scaffolds fabricated with pore-size gradients as a model for studying the zonal organization within tissue-engineered cartilage constructs. Tissue Eng 11:1297–1311.

Woodfield TB, Malda J, de Wijn J, Peters F, Riesle J, van Blitterswijk CA. 2004. Design of porous scaffolds for cartilage tissue engineering using a three-dimensional fiber-deposition technique. Biomaterials 25:4149–4161.

Yates KE, Shortkroff S, Reish RG. 2005. Wnt influence on chondrocyte differentiation and cartilage function. DNA Cell Biol 24:446–457.

Zhang Y, Wang F, Tan H, Chen G, Guo L, Yang L. 2012. Analysis of the mineral composition of the human calcified cartilage zone. Int J Med Sci 9:353–360.

Zhao W, Jin X, Cong Y, Liu Y, Fu J. 2013. Degradable natural polymer hydrogels for articular cartilage tissue engineering. J Chem Technol Biotechnol 88:327–339.

Zhou S, Cui Z, Urban JP. 2008. Nutrient gradients in engineered cartilage: metabolic kinetics measurement and mass transfer modeling. Biotechnol Bioeng 101:408–421.